



Contents lists available at ScienceDirect

Nuclear Inst. and Methods in Physics Research, A

journal homepage: www.elsevier.com/locate/nima

TCAD modeling of radiation-induced defects in 4H-SiC diodes

Philipp Gaggl^{a,b}, Jürgen Burin^a, Andreas Gsponer^{a,b}, Simon-Emanuel Waid^a,
Richard Thalmeier^a, Thomas Bergauer^a*

^a Institute of High Energy Physics of the Austrian Academy of Sciences, Nikolsdorfer Gasse 18, 1050, Vienna, Austria^b TU Wien, Wiedner Hauptstr. 8–10, 1040, Vienna, Austria

ARTICLE INFO

Keywords:

Silicon carbide
Radiation damage to detector materials (solid state)
TCAD
Numerical simulations
Defect states

ABSTRACT

4H silicon carbide (SiC) has several advantageous properties compared to silicon (Si) making it an appealing detector material, such as a larger charge carrier saturation velocity, bandgap, and thermal conductivity. While the current understanding of material and model parameters suffices to simulate unirradiated 4H-SiC using TCAD software, configurations accurately predicting performance degradation after high levels of irradiation due to induced traps and recombination centers do not exist. Despite increasing efforts to characterize the introduction and nature of such defects, published results are often contradictory. This work presents a bulk radiation damage model for TCAD simulation based on existing literature and optimized on measurement results of neutron-irradiated 4H-SiC pad diodes. Experimentally observed effects, such as flattening of the detector capacitance, loss of rectification properties, and degradation in charge collection efficiency, are reproduced. The EH_4 center is suggested as a major lifetime killer in 4H-SiC, while the still controversial assumption of the $\text{EH}_{6,7}$ deep-level being of donor type is reinforced.

1. Introduction

Future high-energy physics (HEP) experiments ought to sustain unprecedented radiation fluences up to $10^{18} \text{ n}_{\text{eq}}/\text{cm}^2$ (1 MeV neutron equivalent according to NIEL hypothesis [1]) at innermost detector layers, while low material budget requirements forbid materials like cooling pipes. Due to its unique properties and recent improvements in manufacturing, research in 4H silicon carbide (4H-SiC) as high-energy particle detector material has been rekindled [2,3]. A venture necessitating simulations via technology computer-aided design (TCAD) software. Despite a multitude of studies on performance degradation of, and defect formation in 4H-SiC after irradiation, no TCAD model to accurately reproduce these findings exists to the best of our knowledge. Utilizing the TCAD software Sentaurus [4], this work represents our first results towards developing a comprehensive radiation damage model for 4H-SiC up to high irradiation fluences. Focused solely on bulk defects, literature defect parameters are adapted to reproduce measurements on neutron-irradiated 4H-SiC samples described in [5].

2. Materials and methods

Five planar, $3 \times 3 \text{ mm}^2$ 4H-SiC PiN-diodes with a $50 \mu\text{m}$, high resistive ($20 \Omega \text{ cm}$), epitaxial layer as active detecting region, manufactured and developed at IMB-CNM-CSIC [6], were studied. Four of them were

neutron-irradiated at the TRIGA Mark II reactor at the Atominstut in Vienna at different fluences (Φ), ranging from $5 \times 10^{14} \text{ n}_{\text{eq}}/\text{cm}^2$ to $1 \times 10^{16} \text{ n}_{\text{eq}}/\text{cm}^2$. Detailed information can be found in [7]. The electrical characterization included current (I–V) and capacitance (C–V), as well as charge collection efficiency (CCE) measurements of α -particles in forward and reverse operating bias [5].

Due to the p^{++} -implant and metallization covering the active diode area, the proposed TCAD model considers only bulk defects, neglecting contributions of interface defects and oxide charges. Results of existing literature characterizing radiation-induced defects in 4H-SiC are subject to differing manufacturers and material quality, thus widely dispersed and sometimes contradictory. The ensuing large parameter space served as a starting point for the optimization of individual values to best fit experimental results from [5]. The investigated publications focus on neutron and electron-irradiated 4H-SiC since results compare very well [8–10]. Active defects in the simulation are either intrinsic (D & B) or radiation-induced ($\text{Z}_{1,2}$, $\text{EH}_{6,7}$ & EH_4) via a linear introduction rate ($N_i = f_i \cdot \Phi$). Defect types and cross-sections are assumed constant over the whole range of neutron fluences. Due to the low dark current levels of 4H-SiC, reverse I–V measurements are dominated by electric noise and surface currents, restricting TCAD comparison to forward bias operation. I–V simulations have been conducted in *SDevice*, using an AC Analysis in *Single-Device Mode* to simultaneously obtain C–V

* Corresponding author.

E-mail address: thomas.bergauer@oeaw.ac.at (T. Bergauer).<https://doi.org/10.1016/j.nima.2024.170015>

Received 2 July 2024; Received in revised form 15 October 2024; Accepted 21 October 2024

Available online 28 October 2024

0168-9002/© 2024 Elsevier B.V. All rights reserved, including those for text and data mining, AI training, and similar technologies.

Table 1

Optimized TCAD model parameters: Defect type, activation energy, e^-/h^+ capture cross-sections, and concentration after 1MeV equivalent neutron fluence Φ . E_C and E_V denote the conduction and valence band energy. Additionally, the investigated literature that best fits the respective value, is given.

Defect	Type	E [eV]	σ_e [cm ²]	σ_h [cm ²]	N [cm ⁻³]
Z _{1,2}	Acceptor	$E_C - 0.67$ [16]	$2.0 \cdot 10^{-14}$ [16]	$3.5 \cdot 10^{-14}$ [17]	$5.0 \cdot \Phi$ [8]
EH _{6,7}	Donor	$E_C - 1.60$ [18]	$9.0 \cdot 10^{-12}$ [18]	$3.8 \cdot 10^{-14}$ [18]	$1.6 \cdot \Phi$ [8]
EH ₄	Acceptor	$E_C - 1.03$ [19]	$5.0 \cdot 10^{-13}$ [20]	$5.0 \cdot 10^{-14}$ [8]	$2.4 \cdot \Phi$ [8]
B	Donor	$E_V + 0.28$ [21]	$2.0 \cdot 10^{-15}$ [22]	$2.0 \cdot 10^{-14}$ [8]	$1.0 \cdot 10^{14}$
D	Donor	$E_V + 0.54$ [21]	$2.0 \cdot 10^{-15}$ [22]	$2.0 \cdot 10^{-14}$ [8]	$1.0 \cdot 10^{14}$

data (10 kHz AC-frequency [5]) at equal simulation settings. Obtained field constellations were saved in 50 V steps and used to simulate detection performance, utilizing the *HeavyIon* model to simulate the depth-dependent energy loss of α -particles corresponding to the source used in [5]. Applied settings and physics models are described in [11–13].

3. Results

Table 1 summarizes the optimized defects of the TCAD irradiation model and their respective parameters, as well as publications best fitting the final obtained values. Aside from the widely known *major lifetime killers* in 4H-SiC (Z_{1,2} & EH_{6,7}), the EH₄ defect cluster proved to be crucial as well. As discussions about the type of the EH_{6,7} defect continue, the presented model strongly suggests it to be of donor-type [14,15]. Aside from slight improvements in C-V conformity, the intrinsic Boron centers (B & D) do not affect results.

Fig. 1 depicts measured and simulated I–V results in forward bias. The model accurately predicts the 4H-SiC device losing its rectifying properties with increasing irradiation, allowing for forward biasing up to high voltages [5,10]. Absolute values are in good agreement with experiments, despite increasingly underestimating current levels with rising fluence, which may be attributed to surface currents omitted in the model. Simulations suggest a high concentration of trapped holes (EH_{6,7}) near the top, and electrons (EH₄) near the bottom due to their respective abundance within the p⁺⁺ implant and the n⁺ buffer layer [6]. The resulting potential forms an electric field barrier that suppresses current flow and increases with the irradiation fluence. The current level in this confinement is mainly determined by the majority carrier trap (Z_{1,2} & EH₄) concentration. At sufficient bias, defects on either side become fully occupied, increasing the respective carrier lifetimes and restoring conducting properties, as can be observed for the lowest fluence in Fig. 1. The resulting rectification voltage is determined by the EH₄ concentration, as it reaches full occupations earlier. Not displayed are reverse I–V simulations, which show a slight increase in leakage current with irradiation fluence that remains below an order of magnitude increase. Although in agreement with other studies [7,10], no further conclusion can be made, as simulated currents are multiple orders of magnitude below the experimental measurement limitations of around 100 fA.

The detector capacitance has been shown to *flatline* after irradiation, adopting a constant value across forward and reverse bias [5,10]. Fig. 2 displays measured and simulated reverse $1/C^2$ data. While defect parameters were adjusted mainly to agree with I–V measurements, C–V simulations reproduce experimental results, with slight deviations most likely originating inaccuracies in the simulated initial doping profile.

Measured and simulated charge collection efficiency (CCE), obtained by scaling signal areas to that of the unirradiated counterpart, are shown in Fig. 3. The radiation-induced performance degradation can be reproduced well at low irradiation, while deviations increase towards higher fluences.

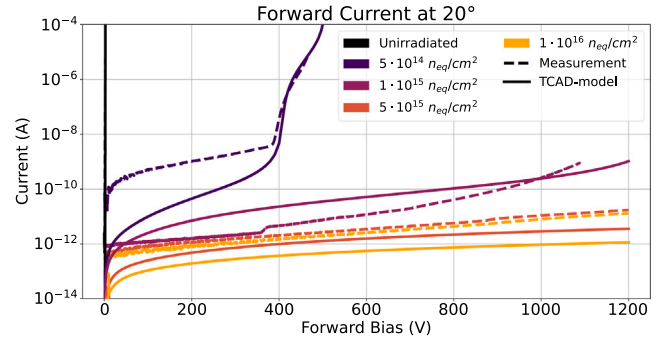


Fig. 1. Forward bias I–V measurements [5] vs. simulation.

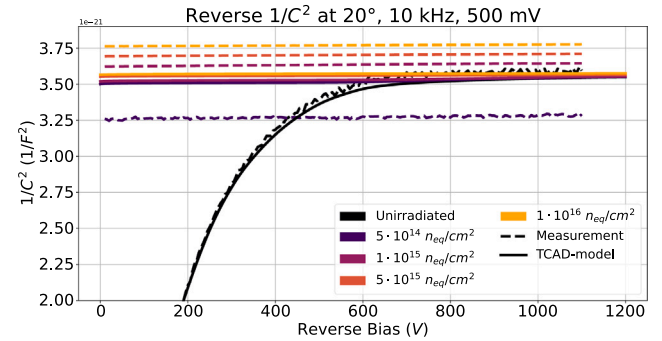


Fig. 2. Reverse bias $1/C^2$ -V measurements [5] vs. simulation. The unirradiated case (black) represents the characteristic depletion of a PiN-diode under reverse operation, the extracted full depletion voltage is 325 V.

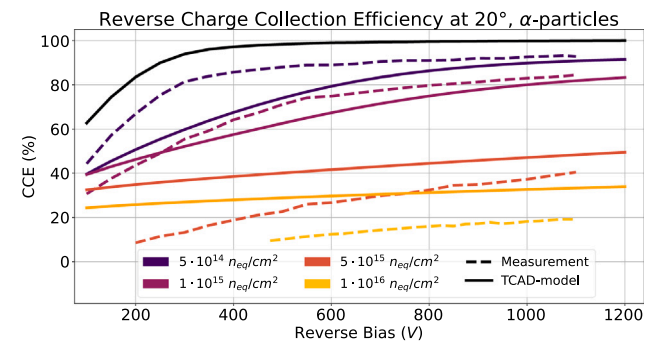


Fig. 3. Reverse bias CCE measurements [5] vs. simulation.

4. Conclusions and outlook

A first step towards a comprehensive TCAD model for radiation-induced bulk defects in 4H-SiC has been developed. Simulated data agrees well with measurements on neutron-irradiated 4H-SiC diodes. While absolute I–V values deviate with increasing irradiation fluence,

the loss of rectification properties after irradiation can be reproduced. Suggested to be originating from major shifts within the internal electric field structure due to charge separation, the deep-level defects EH_4 and $\text{EH}_{6,7}$ are identified as driving forces behind this process. Furthermore, the model reinforces recent and still discussed proposals of the $\text{EH}_{6,7}$ center being of donor type while also introducing the EH_4 defect as a significant lifetime killer in 4H-SiC, next to the established $\text{Z}_{1,2}$ center. Other trends, such as a flattening detector capacitance and a degradation in charge collection efficiency after irradiation, are recreated and agree well with experimental results at lower fluences, increasingly deviating at higher fluences. Further and more extensive irradiation studies on various types of 4H-SiC devices are needed to confirm and improve the presented simulation model, as well as to expand it towards interface defects and oxide charges. Additional 4H-SiC samples, currently under production, are scheduled for an extensive irradiation campaign, which will include various irradiation sources and is planned to cover a wide fluence range of 10^{13} $n_{\text{eq}}/\text{cm}^2$ to 10^{18} $n_{\text{eq}}/\text{cm}^2$.

Declaration of competing interest

The authors declare that they have no known competing financial interests or personal relationships that could have appeared to influence the work reported in this paper.

Acknowledgments

This project has received funding from the Austrian Research Promotion Agency FFG, Austria, grant numbers 883652 and 895291. Production and development of the 4H-SiC samples was supported by the Spanish State Research Agency (AEI) and the European Regional Development Fund (ERDF), ref. RTC-2017-6369-3.

References

- [1] M. Moll, Radiation Damage in Silicon Particle Detectors: Microscopic Defects and Macroscopic Properties (Ph.D. thesis), Hamburg U., 1999.
- [2] J. Coutinho, et al., Silicon carbide diodes for neutron detection, *NIM-A* 986 (2021) 164793.
- [3] F. Nava, et al., Silicon carbide and its use as a radiation detector material, *Meas. Sci. Technol.* 19 (10) (2008) 102001.
- [4] Synopsys Sentaurus TCAD Ver. V-2023.09, Synopsys, Inc., 2024, URL: <https://www.synopsys.com/home.aspx>.
- [5] A. Spöner, et al., Neutron radiation induced effects in 4H-SiC PiN diodes, *J. Instrum.* 18 (11) (2023) <http://dx.doi.org/10.1088/1748-0221/18/11/C11027>.
- [6] J. Raffi, et al., Four-quadrant silicon and silicon carbide photodiodes for beam position monitor applications: electrical characterization and electron irradiation effects, *J. Instrum.* 13 (01) (2018) <http://dx.doi.org/10.1088/1748-0221/13/01/C01045>.
- [7] P. Gaggl, et al., Charge collection efficiency study on neutron-irradiated planar silicon carbide diodes via UV-TCT, *NIM-A* 1040 (2022) <http://dx.doi.org/10.1016/j.nima.2022.167218>.
- [8] P. Hazdra, et al., Point defects in 4H-SiC epilayers introduced by 4.5 MeV electron irradiation and their effect on power JBS SiC diode characteristics, in: *Gettering and Defect Engineering in Semiconductor Technology XV*, in: *Solid State Phenomena*, vol. 205, Trans Tech Publications Ltd, 2014, pp. 451–456, <http://dx.doi.org/10.4028/www.scientific.net/SSP.205-206.451>.
- [9] P. Hazdra, J. Vobecký, Radiation Defects Created in n-Type 4H-SiC by Electron Irradiation in the Energy Range of 1–10 MeV, *Phys. Status Solidi (a)* 216 (17) (2019) 1900312, <http://dx.doi.org/10.1002/pssa.201900312>.
- [10] J.M.o. Rafi, Electron, neutron, and proton irradiation effects on SiC radiation detectors, *IEEE Trans. Nucl. Sci.* 67 (12) (2020) 2481–2489, <http://dx.doi.org/10.1109/TNS.2020.3029730>.
- [11] P. Gaggl, Improving TCAD Simulation of 4H Silicon Carbide Particle Detectors, Presented at 42rd RD50 Workshop, CERN, Switzerland, 2023, <https://indico.cern.ch/event/1334364/contributions/5672054/>.
- [12] Synopsys Sentaurus TCAD, Tips & tricks 2. Simulating wide-bandgap semiconductors with sentaurus device, 2020, https://spdocs.synopsys.com/dow_retrieve/qsc-r/seg/sentaurus/R-2020.09/training/sentaurus_training/tips/tips_2.html.
- [13] Synopsys Sentaurus TCAD, Sentaurus device 15. Special focus: 4H-SiC PiN device breakdown simulation, 2020, https://spdocs.synopsys.com/dow_retrieve/qsc-r/seg/sentaurus/R-2020.09/training/sentaurus_training/sd/sd_15.html#5.
- [14] I.D. Booker, et al., Donor and double-donor transitions of the carbon vacancy related $\text{EH}_{6,7}$ deep level in 4H-SiC, *J. Appl. Phys.* 119 (2016) 235703, <http://dx.doi.org/10.1063/1.4954006>.
- [15] M.E. Bathen, et al., Dual configuration of shallow acceptor levels in 4H-SiC, *Mater. Sci. Semicond. Process.* 177 (2024) 108360, <http://dx.doi.org/10.1016/j.mssp.2024.108360>.
- [16] P.B. Klein, Identification and carrier dynamics of the dominant lifetime limiting defect in n- 4H-SiC epitaxial layers, *Phys. Status Solidi (A)* 206 (10) (2009) 2257–2272, <http://dx.doi.org/10.1002/pssa.200925155>.
- [17] P.B. Klein, et al., Lifetime-limiting defects in n- 4H-SiC epilayers, *Appl. Phys. Lett.* 88 (5) (2006) 052110, <http://dx.doi.org/10.1063/1.2170144>.
- [18] T. Knezevic, et al., Boron-related defects in N-type 4H-SiC Schottky barrier diodes, *Materials* 16 (9) (2023) <http://dx.doi.org/10.3390/ma16093347>.
- [19] G. Alfieri, et al., Annealing behavior between room temperature and 2000°C of deep level defects in electron-irradiated n-type 4H silicon carbide, *J. Appl. Phys.* 98 (4) (2005) 043518, <http://dx.doi.org/10.1063/1.2009816>.
- [20] I.D. Booker, et al., Carrier lifetime controlling defects $\text{Z}_{1/2}$ and RB_1 in standard and chlorinated chemistry grown 4H-SiC, *Cryst. Growth Des.* 14 (8) (2014) 4104–4110, <http://dx.doi.org/10.1021/cg5007154>.
- [21] I. Capan, T. Brodar, Majority and minority charge carrier traps in n-type 4H-SiC studied by junction spectroscopy techniques, *Electronic Materials* 3 (1) (2022) 115–123, URL: <https://www.mdpi.com/2673-3978/3/1/11>.
- [22] P.B. Klein, et al., Slow de-trapping of minority holes in n-type 4H-SiC epilayers, *Phys. Status Solidi (A)* 208 (12) (2011) 2790–2795, <http://dx.doi.org/10.1002/pssa.201127260>.